AFRL-ML-WP-TP-2007-461

THERMO-OXIDATIVE BEHAVIOR OF HIGH TEMPERATURE PMR-15 RESIN AND COMPOSITES (Postprint)

G.P. Tandon, K.V. Pochiraju, and G.A. Schoeppner

FEBRUARY 2007

Approved for public release; distribution is unlimited.

STINFO COPY

MATERIALS AND MANUFACTURING DIRECTORATE
AIR FORCE RESEARCH LABORATORY
AIR FORCE MATERIEL COMMAND
WRIGHT-PATTERSON AIR FORCE BASE, OH 45433-7750

NOTICE

Using Government drawings, specifications, or other data included in this document for any purpose other than Government procurement does not in any way obligate the U.S. Government. The fact that the Government formulated or supplied the drawings, specifications, or other data does not license the holder or any other person or corporation; or convey any rights or permission to manufacture, use, or sell any patented invention that may relate to them.

This report was cleared for public release by the Air Force Research Laboratory Wright Site (AFRL/WS) Public Affairs Office (PAO) and is releasable to the National Technical Information Service (NTIS). It will be available to the general public, including foreign nationals.

THIS TECHNICAL REPORT IS APPROVED FOR PUBLICATION.

*//signature//

GREGORY A. SCHOEPPNER, Research Engineer
Structural Materials Branch
Nonmetallic Materials Division

//signature//

KEITH B. BOWMAN, Acting Branch Chief
Structural Materials Branch
Nonmetallic Materials Division

//signature//

SHASHI K. SHARMA, Acting Deputy Chief
Nonmetallic Materials Branch
Materials and Manufacturing Directorate

This report is published in the interest of scientific and technical information exchange and its publication does not constitute the Government's approval or disapproval of its ideas or findings.

*Disseminated copies will show "//signature//" stamped or typed above the signature blocks.

REPORT DOCUMENTATION PAGE

Form Approved
OMB No. 0704-0188

1. REPORT DATE *(DD-MM-YY)*	2. REPORT TYPE	3. DATES COVERED *(From - To)*
February 2007	Conference paper postprint	

4. TITLE AND SUBTITLE
THERMO-OXIDATIVE BEHAVIOR OF HIGH TEMPERATURE PMR-15 RESIN AND COMPOSITES (Postprint)

5a. CONTRACT NUMBER
FA8650-05-D-5052

5b. GRANT NUMBER

5c. PROGRAM ELEMENT NUMBER
62102F

6. AUTHOR(S)
G.P. Tandon (UDRI)
K.V. Pochiraju (Stevens Institute of Technology)
G.A. Schoeppner (Structural Materials Branch (AFRL/MLBC))

5d. PROJECT NUMBER
4349

5e. TASK NUMBER
RG

5f. WORK UNIT NUMBER
M03R1000

7. PERFORMING ORGANIZATION NAME(S) AND ADDRESS(ES)

UDRI
300 College Park
Dayton OH 45469-0168

Stevens Institute of Technology
Dept. of Mechanical Engineering
Hoboken, NJ 07030

Structural Materials Branch (AFRL/MLBC)
Nonmetallic Materials Division
Materials and Manufacturing Directorate
Air Force Research Laboratory, Air Force Materiel Command
Wright-Patterson AFB, OH 45433-7750

8. PERFORMING ORGANIZATION REPORT NUMBER

9. SPONSORING/MONITORING AGENCY NAME(S) AND ADDRESS(ES)
Materials and Manufacturing Directorate
Air Force Research Laboratory
Air Force Materiel Command
Wright-Patterson AFB, OH 45433-7750

10. SPONSORING/MONITORING AGENCY ACRONYM(S)
AFRL-ML-WP

11. SPONSORING/MONITORING AGENCY REPORT NUMBER(S)
AFRL-ML-WP-TP-2007-461

12. DISTRIBUTION/AVAILABILITY STATEMENT
Approved for public release; distribution is unlimited.

13. SUPPLEMENTARY NOTES
PAO Case Number: AFRL/WS 07-0262, 14 February 2007. Presented at the 2nd International Conference on Recent Advances in Composite Materials (ICRACM-2007), 20 Feb. 2007, New Delhi, India.

14. ABSTRACT
The present study examines the thermo-oxidative behavior of high-temperature polymer matrix composite (HTPMC) materials. Thermo-oxidative aging in neat resin is simulated with a diffusion-reaction model in which temperature, oxygen concentration, and weight loss effects are considered. The thermo-oxidative behavior of the composite, on the other hand, is significantly different from that of the constituents as the composite microstructure, including the fiber/matrix interphase/interface, introduces anisotropy in the diffusion and oxidation behavior. Unit cell analyses are carried out using three-dimensional finite element analysis of repeated volume elements representing the fiber, matrix and interphase regions, and the resin oxidation model. Parametric studies illustrating the anisotropy in the oxidative region growth and the effect of fiber and interphase diffusivity on the oxidation layer growth are discussed. It is suggested that fiber-matrix debonding could provide additional diffusion paths to explain the extent of observed anisotropic oxidation growth.

15. SUBJECT TERMS
Thermo-oxidation, anisotropic, diffusion, reaction, aging, damage

16. SECURITY CLASSIFICATION OF:			17. LIMITATION OF ABSTRACT:	18. NUMBER OF PAGES	19a. NAME OF RESPONSIBLE PERSON (Monitor)
a. REPORT	b. ABSTRACT	c. THIS PAGE			Gregory Schoeppner
Unclassified	Unclassified	Unclassified	SAR	50	19b. TELEPHONE NUMBER *(Include Area Code)* (937) 255-9019

Standard Form 298 (Rev. 8-98)
Prescribed by ANSI Std. Z39-18

Thermo-oxidative Behavior of High Temperature PMR-15 Resin and Composites

G.P. Tandon[a*], K.V. Pochiraju[b] and G.A. Schoeppner[c]

[a] University of Dayton Research Institute, 300 College Park, Dayton, OH 45469-0168, USA

[b] Stevens Institute of Technology, Department of Mechanical Engineering, Hoboken, NJ 07030, USA

[c] US Air Force Research laboratory, AFRL/MLBC, Wright-Patterson Air Force Base, OH 45433, USA

Abstract.

The present study examines the thermo-oxidative behavior of high-temperature polymer matrix composite (HTPMC) materials. Thermo-oxidative aging in neat resin is simulated with a diffusion-reaction model in which temperature, oxygen concentration and weight loss effects are considered. The thermo-oxidative behavior of the composite, on the other hand, is significantly different from that of the constituents as the composite microstructure, including the fiber/matrix interphase/interface, introduces anisotropy in the diffusion and oxidation behavior. Unit cell analyses are carried out using three-dimensional finite element analysis of repeated volume elements representing the fiber, matrix and interphase regions, and the resin oxidation model. Parametric studies illustrating the anisotropy in the oxidative region growth and the effect of fiber and interphase diffusivity on the oxidation layer growth are discussed. It is suggested that fiber-matrix debonding could provide additional diffusion paths to explain the extent of observed anisotropic oxidation growth.

Keywords: thermo-oxidation, anisotropic, diffusion, reaction, aging, damage

- Corresponding author
  Email address: G.Tandon@wpafb.af.mil

1. Introduction

Polymer matrix composites (PMCs) used in aerospace high temperature applications, such as turbine engines and engine exhaust washed structures, have limited life due to environmental degradation. Predicting the service life of composite structures subjected to mechanical, high temperature, moisture, and corrosive conditions is challenging due to the complex physical, chemical, and thermo-mechanical mechanisms evolving with time in the constituent phases. While the time-dependent physical, chemical, and damage-induced degradation mechanisms have been studied for some resin systems, polymer composite thermal oxidation studies from a mechanistic perspective are nascent. Notable exceptions to this are the recent works of Colin and Verdu [1], Colin, et al. [2], Wang and Chen [3], Pochiraju, et al. [4], Tandon, et al. [5], and past work by Skontorp, et al. [6], Wise, et al. [7], and McManus, et al. [8]. Equally important are the experimental characterization efforts by such groups as Bowles, et al., [9]; Tsuji, et al., [10]; Abdeljaoued [11], and Schoeppner, et al. [12]. Current emphasis is on the implementation and extension of multiscale models to represent the polymer behavior/properties as a function of the degradation state to include chemical degradation kinetics, micromechanical models with time-dependent polymer constitutive relationships, and on ply-level and laminate level models to predict structural behavior. The behavior of the composite will thus be dependent on its current chemical, physical, and mechanical state as well as its service history. This multidisciplinary modeling approach will provide generalizable analytical and design tools for realistic prediction of performance, durability, and use life of HTPMCs.

2. Experimental Characterization and Observations

The attributes of the oxidation process of high temperature polymer and polymer composites vary dependent on the chemistry of the polymers being tested. The primary focus of the discussion in this work is on predicting isothermal oxidative aging of unitape laminates with particular focus on the composites utilizing PMR-15 high temperature polymer. Additionally, the reinforcement is limited to PAN-based carbon fibers. PMR-15 is a widely-used addition polyimide with a maximum service temperature of approximately 288ºC. Among the class of high temperature polymers are the bismaleimides, Avimid-N, thermosetting polyimides (AFR700B, LARC RP46) and phenylethynyl-terminated polyimides (PETI-5, AFR-PE-N) resin systems. Each of these material systems has unique degradation reactions, mechanisms, and kinetics particular to their chemical structure. Although experimental observations and predictions of the behavior of PMR-15 neat resin and composites are not necessarily representative of the behavior of these other high temperature polymer material systems, the modeling methodology and procedures for determining material parameters may be directly applicable to predicting their behavior.

2.1 Resin Oxidation

Recent studies [1,3,9,13,14] document the growth of the thermo-oxidative layer in PMR-15 resin and the changes in elastic moduli and chemical composition resulting from isothermal aging. It has been observed for PMR-15 that the polymer degradation occurs mainly within a thin surface layer that develops and grows during thermal aging.

In our work, for both the neat polymer and composite specimens that were used to monitor the propagation of oxidation, samples were dry-sectioned from the aged larger specimen, as shown in Fig. 1, potted in 828-D230 epoxy resin, and cured at room temperature for three days. This sectioning procedure allowed monitoring of four of the exposed free-surfaces of the large specimen. The large specimen was subsequently placed back in the oven to continue the aging process. The diamond blade used to section these samples was washed with acetone and wiped clean with paper towels prior to cutting to minimize the amount of contamination from the cutting wheel. The specimens were then wet-sanded with 600-grit sandpaper and distilled water and polished using a 0.3-micron alumina polishing media. Since the oxidized layer forms on all exposed free-surfaces and propagates to the interior of the sample, the oxidized region is easily seen in the cross section.

Fig. 2 shows a photomicrograph of a PMR-15 neat resin specimen isothermally aged in air under elevated pressure (0.414 MPa) at 288^0C for a period of 175 hrs. The figure clearly shows the oxidized region (much like a picture frame) on the two adjacent exposed free surfaces of the specimen. The dark shaped region between the outer oxidized layer and interior unoxidized region is a transition region, which is the active "reaction" or "process" zone. These observations allow easy measuring and characterization of the oxidized layer and the transition regions as a function of aging temperature and time. Fig. 3 shows the evolution of the oxidized layer and the active "reaction" zone thicknesses as a function of aging time for PMR-15 resin aged at 288^0C. The thickness of the oxidized layer is seen to approach a plateau value as the oxidation

growth rate reduces considerably for longer aging time periods, whereas the thickness of the active "reaction" zone remains nearly constant for the aging times considered.

The rate of oxidation is sensitive to the partial pressure of oxygen at the specimen surface and acceleration can be achieved by increasing the air pressure and thus the partial pressure of oxygen within the aging chamber (e.g., Ciutacu, et al. [15], Tsotsis, et al. [16]). Recent work by Tandon, et al. [17] examined the use of elevated pressure in conjunction with a realistic use temperature to accelerate the rate of thermo-oxidative degradation in PMR-15 resin. It was observed that the elevated pressure aging of the PMR-15 neat resin presumably had a significant effect on the rate of diffusion of oxygen into the specimen, accelerating the oxidation process and allowing the oxygen to diffuse deeper into the interior of the specimens. This results in greater oxidation layer thicknesses than are achievable in ambient air pressure environments as shown in Fig. 4.

2.2 Fiber oxidation

The effects of service temperatures and oxidation on the mechanical properties of high-temperature polymer composites are primarily manifested in the polymer-dominated properties, namely, the transverse properties (perpendicular to the fiber direction) and the shear properties. However, the fiber-dominated properties may be affected by degradation of the fiber and deterioration of the fiber-matrix interface. This may be particularly true for composites with glass fibers in which magnesium and sodium can leach out from the fiber and possibly contribute to polymer/interface degradation. It is reported that graphite fibers containing significant amounts of sodium

and potassium as contaminants are less thermo-oxidatively stable than graphite fibers with very low alkali metal contents [18,19].

The relative oxidative stability of three polyacrylonitrile (PAN)-based carbon fibers, namely, T650-35, G30-500 and IM7, was recently determined [20] by comparing the percent weight lost during isothermal elevated temperature exposure. As an example, Fig. 5 shows a comparison of the weight loss normalized by the surface areas of G30-500 carbon fiber and PMR-15 neat resin aged at 288^0C. Note that the normalized fiber weight loss is almost negligible compared to that of neat resin over 2000 hrs of aging. Thus, even though the carbon fiber could lose a significant weight fraction with aging at elevated temperature (as much as 10% for G30-500 fibers after 2000 hrs of aging at 288^0C), the weight loss normalized by the fiber surface area is negligible because of the large surface area of bare fibers. Futher, note that aging of the bare fibers may not necessarily be representative of the behavior of the in-situ fibers embedded in the matrix because the exposed surface area of the fibers in the composite is only a very small percentage of the total surface area of the fibers.

While it has been established that the fibers account for only a minimal amount of the total weight loss for HTPMCs, nevertheless, the role of fibers in the composite oxidation process, in particular their role in transporting oxygen into the composite, is not fully understood. Extruded PAN carbon fibers exhibit a preferred orientation in which the graphitic layers may extend for thousands of angstroms and extend straight for hundreds of angstroms parallel to the fiber axis providing high-strength and high-stiffness along the fiber axis direction. It is very likely that the diffusivity of the fibers

will also be anisotropic in nature. Unfortunately, experimental measures of carbon fiber diffusivity have not been obtained. In addition, while carbon fibers may be more resistant to oxidation and have longer relaxation times than the polymer matrix, the mechanical performance of the fiber-matrix interface at high temperatures may be critical to the evolution of damage and composite failure. The properties of the fiber-matrix interface or interphase region are a function of the interaction of the fiber and matrix during the manufacturing process, the chemical compatibility of fiber, and the sizing (if applicable) on the fiber. The role of the fiber-matrix interface in the composite oxidation process will be discussed in subsequent sections.

2.3 Composite oxidation

The anisotropic oxidative response of PMCs was first documented by Nelson [21] when he observed that the oxidation process is sensitive to the surface area for the different test specimen geometries that he investigated. He found that the dominant degradation mechanism for the graphite/polyimides is oxidation of the matrix at the laminate edges. Additionally, the materials degraded preferentially at the specimen surface perpendicular to the fiber (axial surface), and the rate of oxidation is hastened by microcracks opening on the axial surface increasing the surface area for oxidation. The anisotropic nature of oxidation in HTPMCs has also been observed by numerous other investigators including the works of Nam and Seferis [22] and Skontorp, et al. [6]. Although it is well documented that unidirectional composites preferentially oxidize in the fiber direction [21-23], details of the rate of oxidation propagation in the orthogonal directions of unidirectional composites is not well documented.

Dark-field microscopy was utilized [12] to monitor the oxidation propagation rates in both the axial direction (along the fiber) and the transverse direction (transverse to the fibers) of unidirectional G30-500/PMR-15 composites aged in air at 288ºC. Fig. 6 shows (a) the original stitched micrograph, and (b) an enhanced micrograph that clearly distinguishes the white oxidized material from the black unoxidized material. The oxidation layer appears as a frame around the composite specimen just as seen in aged neat resin PMR-15 samples in Fig. 2. The specimen of Fig. 6 aged for 197-hours is shown to have only minimal oxidation transverse to the fibers, but has moderate oxidation development in the axial direction. The method of enhancing the micrograph consists of constructing (using Adobe Photoshop 7.0) a complete image of the entire composite by stitching together individual micrographs using standard light microscopy in the grayscale mode. Once the image is constructed, the apparent light oxidized region is best fit in the lab mode to a pure white specified as having a lightness value of 100, while the remaining unoxidized regions of the image are given a lightness value of zero. Thus, this image processing creates exactly two distinct grayscale colors: black and white.

Fig. 7 shows enhanced micrographs of G30-500/PMR-15 unidirectional composites after 407, 1200 and 2092 hours of aging at 288ºC that clearly show that oxidation substantially increases in both the axial and transverse directions with aging time. Next, the overall level of oxidation is quantified by measuring the percentage of the specimen cross-sectional surface area that is oxidized. Using constructed enhanced micrograph images, a histogram of the images are used to determine the ratio of white to black pixels, and the ratios are used to quantify the amount of surface area of the composite

cross section that is oxidized. Quantification of the oxidation area using this process is a two-dimensional representation and does not account for stochastic variations of the oxidized cross section through the thickness of the specimen. Fig. 8 shows the average of the extent of the axial oxidation along the fiber direction as a function of aging time at 288ºC. The figure also includes the average of the extent of the transverse oxidation from the enhanced micrographs. Fig. 8 clearly shows the dominance of the axial oxidation degradation as compared to the transverse degradation in composites which can be attributed to the higher effective diffusivity on the axial surfaces. Fig. 9 compares the oxidation growth in the transverse direction of the composite to the oxidation growth in neat resin PMR-15. It appears that the presence of fibers may initially retard growth of oxidation in the transverse directions. Figs. 8 and 9 clearly show the significant differences between the oxidative behavior of the constituents as compared to the composite owing to the fiber-matrix microstructure that may cause increases in diffusion and reaction rates.

Numerous researchers have attributed the anisotropic diffusivity of unidirectional laminates to the preferential oxidation along the fiber-matrix interface or along the interphase region[1]. However, the interphase region is a very small volume percentage of the composite and a very small area fraction of the surface area. It is questionable that the diffusion of oxygen through and subsequent oxidation of the interphase region by itself can have such a significant effect on the composite oxidation process.

[1] Although fiber-matrix interface and fiber-matrix interphase are often used interchangeably, we formally define the fiber-matrix interface as the two-dimensional surface defined by the common fiber and matrix surfaces. We define the fiber-matrix interphase as the three-dimensional matrix region directly around the fiber that may have properties distinct from the bulk matrix properties.

More likely, the rapid oxidation rate along the fiber length indicates that in addition to diffusion of oxygen from the specimen surface to the oxidation front, the interphase region has a supplemental oxygen path or source. Two possible mechanisms or scenarios for the supplemental oxygen source to the interphase can be considered. Firstly, if oxidation in the interphase region leads to early fiber-matrix interface debond, the debond provides a pathway for oxygen to penetrate deeper into the composite. Knowing that there are residual curing stresses at the fiber-matrix interface, it is likely that such a scenario would entail the interface debond propagating along with the oxidation front. The second scenario is that the oxygen diffuses into the composite along the fiber and to the fiber-matrix interface at a rate much greater than through the neat resin or interphase. Based on the anisotropic oxidation behavior of unidirectional composites, the axial diffusivity of the fibers would have to be much greater than the diffusivity of the resin. Unfortunately, quantitative measures of the diffusivity of carbon fibers are lacking. Although one might anticipate that the bulk diffusivity of carbon is representative of that of the PAN fibers, this would only be the case if the morphology of the fibers and bulk carbon match which in general is not the case.

3. Polymer Oxidation Modeling

The thermo-oxidation model for the polymeric matrix used in this study has been described in detail [4,5]. Thermo-oxidative aging was simulated with a diffusion/reaction model in which temperature, oxygen concentration and weight loss effects were considered. Fig. 10 describes the three-region model in which the surface oxidative layer is separated from the unoxidized polymer with an active reaction zone. As oxygen diffuses

through the polymer, it is consumed by the oxidation reaction. Once a region is fully oxidized, oxygen can diffuse through it and oxidation begins in the adjoining region. This creates three distinct zones. Closest to the oxygen source is a region of completely oxidized polymer. This is followed by the transition region, where oxidation is actively occurring, and finally by the unoxidized interior of the material. Although this three-phase description is analogous to the two-phase models (or skin/core models) described by Nam and Seferis [22], the description of three phases enables extension to situations with high conversion ratios in which the constancy of the substrate concentration is no longer valid and the substrate depletion leads to an auto-retardation of the oxidation kinetics. A practical consequence is a decrease of the oxidation rate in the superficial (region I) layers of the specimen, where the high conversion ratios are firstly reached, which leads to a moving of the oxidation front towards the specimen core. Such an extension was proposed by Colin, et al. [24,25] and successfully applied to the thermal oxidation of amine cross-linked epoxy and bismaleimide resins.

The molar concentration of oxygen at any material point of a constituent material, $C(\bar{x},t)$, is determined by the diffusion reaction equation (Eq. 1).

$$\frac{dC(\bar{x},t)}{dt} = \left[D^*(\phi,T)\right]\nabla^2 C(\bar{x},t) - R^*(C) \qquad (1)$$

where D^* is the diffusivity and $R^*(C)$ represents the oxidation reaction rate function in the material. The exposed boundaries are subject to the oxygen sorption as governed by the Henry's Law. The exposed boundaries are therefore assigned a molar concentration value equal to C^s and oxygen flow across symmetry boundaries is set to zero (Eq. 2). A

negligible initial concentration ($\varepsilon \sim$1e-7 mol/m^3) is assumed through out the domain to avoid numerical difficulties.

$$\begin{aligned} C &= C^S \text{ on the exposed boundaries} \\ \nabla C.n &= 0 \text{ on symmetry boundaries} \\ C(x,0) &= \varepsilon \end{aligned} \tag{2}$$

We introduce an oxidation state parameter, ϕ, which tracks the progress of the oxidation reaction. ϕ varies from $\phi = 1$ for unoxidized state to $\phi = \phi_{ox}$ for completely oxidized state. The determination of ϕ_{ox} value is explained in earlier papers [4,5]. The reaction rate function $R^*(C)$ is influenced by the temperature *T*, available oxygen concentration *C*, and is also a function of the polymer substrate oxidation state variable ϕ as shown in Eq. 3

$$R^*(C) = g(\phi)R(C,T) \tag{3}$$

where $g(\phi)$ describes the reaction rate dependence on the oxidation state variable, and $R(C,T)$ defines the reaction rate dependence on the concentration and temperature. The reaction kinetics are modeled following Colin, et al. [24,25] and Abdeljaoued [11] in which a constant saturation reaction rate R_o is the maximum reaction rate when reaction is not oxygen starved (Eq. 4). The saturation reaction rate is temperature dependent and an Arrhenius relationship is typically assumed for the temperature dependence,

$$\begin{aligned} R(C,T) &= R_0(T)\frac{2\beta C}{1+\beta C}\left(1-\frac{\beta C}{2(1+\beta C)}\right) \\ R_0(T) &= R_0^{'}e^{\frac{-R_a}{RT}} \end{aligned} \tag{4}$$

where the parameter β nondimensionalizes the concentration field, $R_0^{'}$ is the rate constant, and R_a is the activation parameter. Eq. 5 shows the diffusivity of an oxidizing constituent. The diffusivity will depend upon the oxidation state and temperature. Therefore, two values of diffusivity (assuming isotropic diffusivity, scalar diffusivity value is represented instead of the tensor values representing anisotropy) for the oxidized and unoxidized states of the constituent are denoted by *ox* and *un* superscripts, respectively.

$$
\begin{aligned}
D(\phi,T) &= D^{un}(T)\left(\frac{\phi-\phi_{ox}}{1-\phi_{ox}}\right)+D^{ox}(T)\left(\frac{1-\phi}{1-\phi_{ox}}\right)\\
D^{un}(T) &= D_0^{un}\, e^{\frac{-E_a^{un}}{RT}} \qquad (5)\\
D^{ox}(T) &= D_0^{ox}\, e^{\frac{-E_a^{ox}}{RT}}
\end{aligned}
$$

The oxidation state parameter can be directly correlated with the oxidative weight loss (weight loss due to oxidation alone, typically obtained by subtracting the weight loss in an inert – argon - environment from that in an oxidative – air/oxygen – environment). A time dependent proportionality relationship is assumed between the reaction rate and the rate of oxidation as shown in Eq. (6). The reaction rate is assumed to have a linear dependence during the first t_{switch} hours of aging, reducing from α^{max} to a value of α^{min} within t_{switch} hours. The reaction rate after t_{switch} hours is assumed to be constant and equal to lower α^{min}. Again, we refer you to references [4,5] for further details on the rationale of this selection and correlations with the experimental results.

$$\frac{d\phi}{dt} = -\alpha(t)R(C,T)$$

$$\alpha(t) = \begin{cases} \alpha^{\max} - \left(\alpha^{\max} - \alpha^{\min}\right)\left(\dfrac{t}{t_{switch}}\right) : t < t_{switch} \\ \alpha^{\min} : t > t_{switch} \end{cases} \tag{6}$$

The diffusion-reaction system of equations (1-6) can be solved using numerical solutions to differential algebraic equations. The capability to obtain direct measurements of all of the properties of the PMR-15 for each of the three material regions that are needed to populate the parameters for the model is lacking. Therefore, many of the parameters were obtained [4,5] through indirect measurement or correlation with model predictions of the oxidation layer growth obtained at 288ºC.

Fig. 11 shows predictions of the oxidation layer thicknesses for 288°C (550°F), 316°C (600°F), and 343°C (650°F) neat resin PMR-15 specimens based on 288°C (550°F) properties shown in Tables 1-3. The figure shows that the model accurately predicts the 316°C (600°F) and 343°C (650°F) oxidation layer thicknesses, and the temperature dependence of the reaction rate and diffusivity are accurately represented. Further, as mentioned earlier, acceleration of oxidation growth can be achieved by increasing the partial pressure of oxygen within the aging chamber. Since the partial pressure of a gas is directly proportional to the total pressure and in general the solubility of gases increase with increasing pressure, the sorption is expected to increase with increasing pressure. Fig. 12 shows the results of a parametric evaluation of how changes in the sorption affect the predicted oxidation layer thickness. Oxidation layer thickness for neat resin PMR-15 specimens aged at ambient and elevated pressures at

288ºC are also shown in the figure. The predicted oxidation layer thickness increases with increasing oxygen concentration on the boundary and for the sorption value $C^S = 1.25$, there is a good correlation with the pressurized aging data for aging times up to 200 hours. Fig. 13 shows the predicted oxidation layer thickness for predictions up to 800 hours of aging time. The results show good agreement with the experimental data.

4.0 Composite Oxidation Modeling

4.1 Finite Element Framework for Modeling Thermo-Oxidation in Composites

Both two-dimensional and three-dimensional unit cell models capable of discrete crack analysis coupled with thermo-oxidative aged analysis can be used to model and identify the origins of degradation and mechanisms of failure initiation representative of that in unidirectional composites. Traditionally the fibers are assumed to be chemically static for short aging times (this assumption may not be valid for extended aging times) and residual stresses must be taken into account due to the strong coupling between stress, diffusion, and thus aging. Of primary importance is the characterization of the interface/interphase behavior that may have different reaction/diffusion kinetics than the polymer matrix phase of the composite. The fiber-matrix interphase region developed during the composite cure cycle is likely dependent on the fiber surface (unsized or sized) and the composition of the fiber sizing, if it is present.

The diffusion-reaction oxidation model is implemented into a three-dimensional Galerkin Finite Element Analysis (GFEA). The GFEA method is more appropriate for studying structural scale problems than the one- and two-dimensional implementations; however, the computational requirement of the three-dimensional analysis precludes its

use in parametric analyses required for correlation with experimental results and parameter determination. The GFEA requires mesh sizes in the 1-μm scale and time increments in 1-minute steps. A 200-hour oxidation simulation with 100-μm oxidation zone size typically requires problem sizes in the order of 500,000 degrees of freedom (DOF) and 12,000 time steps. The domain, Ω, is discretized by a union of finite elements as $\Omega = \bigcup_{e=1}^{N_e} \Omega^{(e)}$, where $\Omega^i \bigcap \Omega^j = 0$, if $i \neq j$, and N_e is the total number of elements in Ω. The approximate element solution for the concentration C(x,y,z,t) in the diffusion model is defined as

$$C(x,y,z,t) = \left[\Phi(x,y,z)\right]^T \left[C(t)\right] \tag{7}$$

where $\Phi(x,y,z)$ is the spatial interpolation function and C(t) is the time varying nodal concentration values. Using the Galerkin method, i.e. using a weight function same as the interpolation Φ,

$$w = \Phi(x,y,z) \tag{8}$$

the residual for the diffusion-reaction equation (Eq. 7) must vanish as given in Eq. 9

$$\int\!\!\!\int\!\!\!\int \left(\Phi\Phi^T \frac{\partial C(t)}{\partial t} \right) dV + \int\!\!\!\int\!\!\!\int \left(\Phi R^*(C) \right) dV$$

$$+ \int\!\!\!\int\!\!\!\int \left(D_{11}^* \left(\frac{\partial \Phi}{\partial x} \frac{\partial \Phi^T}{\partial x} C(t) \right) + D_{22}^* \left(\frac{\partial \Phi}{\partial y} \frac{\partial \Phi^T}{\partial y} C(t) \right) + D_{33}^* \left(\frac{\partial \Phi}{\partial z} \frac{\partial \Phi^T}{\partial z} C(t) \right) \right) dV = 0 \tag{9}$$

where orthotropic diffusivity is assumed. The superscript * on the diffusivity tensor, D_{ij}^* and reaction rate, $R^*(C)$ is used to indicate that the diffusivity and reaction rate

functions are dependent on the temperature T and oxidation state variable, ϕ . After some mathematical manipulations, Eq. 9 can be written in matrix form as:

$$[\mathbf{C}]\frac{\partial C(t)}{\partial t}+[\mathbf{B}]C(t)+\{\mathbf{R}\}=0 \tag{10}$$

where, the matrices, $[\mathbf{B}]$, $[\mathbf{C}]$, and vector $\{\mathbf{R}\}$ are given by,

$$[\mathbf{B}]=\oint_v\left(D_{11}^{*}\frac{\partial\Phi}{\partial x}\frac{\partial\Phi^{T}}{\partial x}+D_{22}^{*}\frac{\partial\Phi}{\partial y}\frac{\partial\Phi^{T}}{\partial y}+D_{33}^{*}\frac{\partial\Phi}{\partial \mathrm{z}}\frac{\partial\Phi^{T}}{\partial \mathrm{z}}\right)dV \tag{11}$$

$$[\mathrm{C}]=\sum_{e}\int_{\Omega(e)}\Phi\Phi^{T}d\Omega \tag{12}$$

$$\{\mathrm{R}\}=\sum_{e}\int_{\Omega(e)}\Phi R^{*}(C)d\Omega \tag{13}$$

Eq. 10 is discretized by backward Euler method in time domain, where $\Delta t=t^{n+1}-t^{n}$. Therefore, Eq. 10 can be denoted as a system of linear algebraic equations

$$[\mathbf{C}]\left\{\frac{C^{n+1}-C^{n}}{\Delta t}\right\}+[\mathbf{B}]\left\{C^{n+1}\right\}+\{\mathbf{R}\}=0 \tag{14}$$

In summary, the diffusion-reaction equations in their discretized form can be written as:

$$\Re=[\mathbf{D}]\left\{\mathbf{C}^{n+1}\right\}-\{\mathbf{E}\}=0 \tag{15}$$

where,

$$[\mathbf{D}]=[\mathbf{C}]+\Delta t[\mathbf{B}] \tag{16}$$

$$[\mathbf{E}]=[\mathbf{C}]\left\{C^{n}\right\}-\{\mathbf{R}\} \tag{17}$$

Eq. 15 is solved using a direct solution or by minimizing the residual ($\Re$) using an iterative solution such as Jacobi Conjugate Gradient (JCG) iterative method [26] for problems with a large number of degrees of freedom. The time step, Δt, used for this parametric study is 1 minute and the residual is minimized to a root mean square (L^2 norm) value of 1×10^{-8}.

A simple user interface for three-dimensional thermo-oxidative modeling labeled TOM-3D is established to set up the problem domains, material properties and the oxidation rates for each material as shown in Fig. 14. TOM-3D first calculates the concentration profiles and then updates the oxidation state (ϕ) for each element. The oxidation state is taken to be constant over each time step and used for calculation of the ϕ-dependent diffusivity and reaction rates.

Typical meshes used for composite unit cells are shown in Fig. 15. Fig. 15(a) shows a single fiber representative volume element (RVE) with the fiber end exposed to oxidation to simulate axial oxidation growth. It is assumed that the fibers are in a square arrangement, with each fiber having a diameter of 10 μm and a spacing of 12.532 μm (center to center) between adjacent fibers. The RVE is taken to have a nominal fiber volume fraction of 50%, but can be varied easily by changing the FEM mesh. The length of the model is scaled appropriately to the expected oxidation size. The shortest model had a length of 125 μm and the longest 1000 μm in this parametric study. Though not presented in this paper, we have further observed that the simulations for oxidation growth in axial direction using a single fiber model closely match those obtained using multiple fibers with both the fiber ends and axial surface parallel to the

fibers exposed to oxidation. Further, edge effects for fibers located close to the exposed axial surface dissipate within a short time period (~ 40 hours). Since the transverse oxidation for the composite can span multiple fibers, a ten fiber 125 μm x 12.5 μm x 125 μm (shown in Fig. 15(b)) RVE and a 20 fiber 250 μm x 12.5 μm x 125 μm RVE are created for the transverse simulations. The unit-cell size along the length of the fiber (axial direction) is scaled to accommodate the estimated oxidation layer and reaction zone sizes. Note that for this unit cell, both axial and transverse boundaries are exposed to oxidation. Similar to axial oxidation growth, edge effects in transverse simulation become insignificant in a relatively short time period. An interphase region of arbitrary thickness has also been modeled to create a third phase between the fiber and matrix domains. The size and material properties of the interphase region can be parametrically varied. The 10 fiber mesh used has 352,012 elements with 481,761 nodal degrees of freedom (DOF) for concentration and same number for the oxidation state for a total of 963,522 DOFs. The 20 fiber RVE has 447,134 DOFs and 154,486 elements. The 20 fiber RVE is coarser in comparison to 10 fber RVE in order to minimize the computational time. Also, the reaction zone size for the 20 fiber model is expected to be larger because of the selected model parameters, thus, mitigating the need for a finer mesh, as required for the 10 fiber simulation. In the analyses presented in this paper, it is assumed that the fibers do not react with oxygen and are purely diffusive, the interphase diffusivity is parametrically varied (as it is problematic to directly measure interphase diffusivity), and oxidation only occurs in the resin. We also set the sorption value of the fiber and interphase regions to be the same as that of the matrix (C_s = 0.79 mol/m^3). Each of the constituents is modeled explicitly as a separate material and the

interface surfaces at the fiber/interphase and interphase/resin boundaries are assumed to be perfectly diffusive. Resin properties corresponding to that of PMR-15 as given in Tables 1-3 are used.

4.2 Composite Oxidation Studies with Representative Volume Elements (RVE's)

In this section, the diffusivity of the fiber is parametrically varied to evaluate its influence on oxidative growth. Let D_f, D_i and D_m denote the constituent level isotropic diffusivity values of the fiber, interphase region and matrix, respectively. A three-dimensional RVE is used with PMR-15 matrix and an interphase region is initially not included. The oxidation simulation is run for up to 200 hours because steady state oxidation layer growth can be expected at that time. The oxidation state in the model is plotted at various time intervals (25, 50, 100 and 200 hours). Fig. 16 shows the oxidation growth in both axial and transverse directions for various fiber diffusivities and at several hours of exposure. Let the oxidation thickness in the axial and transverse direction be denoted by t_{axial} and t_{trans}, respectively. Similarly, we will denote the thickness of the reaction zone in the axial and transverse direction by l_{axial} and l_{trans}, respectively. The oxidation layer sizes (t_{axial} and t_{trans}) and the reaction zone size (l_{axial} and l_{trans}) are measured using the oxidation state (ϕ) values. The oxidized layer has been considered to have $\phi < 0.181$ (99.5% oxidation) and the unoxidized layer with $\phi > 0.998$ (corresponding to 0.2 % oxidation in the material). These limits are primarily chosen to ensure consistent measurement of the zone sizes throughout the parametric study.

Fig. 16(a) shows the case in which fiber has a very low diffusivity, equivalent to one hundredth that of the oxidized resin, Fig. 16 (b) corresponds to that with a fiber diffusivity of one tenth that of the resin and Fig. 16 (c) shows the oxidation layer size when the fiber diffusivity is about ten times that of the resin. For these simulations, only the diffusive behavior of the fibers is varied whereas both the diffusion and reaction behavior of the resin is considered. When the oxidation state of the resin reaches full oxidation ($\phi=\phi_{ox}=0.18$), the oxidized resin becomes non-reactive and diffusive only. Prior analysis shows that the diffusivity of the oxidized matrix is higher than that of the unoxidized matrix.

When the fiber is less diffusive than the matrix as in cases 16 (a) and 16 (b), the oxidation layer size in both axial and transverse directions is not significantly influenced by the fiber diffusivity. Thus, for low fiber diffusivity values, oxygen diffusion through the fiber becomes insignificant and oxidation is driven by matrix diffusivity alone. However, when the diffusivity of the fiber is higher than that of the matrix as in Case 16 (c), not only is the oxidation layer size larger, the active reaction zone size is also larger indicating the additional supply of oxygen to the active oxidation region of the composite. The effective diffusivity of the oxidized region of the composite controls the growth rate and extent of the oxidation layer.

It is generally believed that the oxidation process in PMR-15 resin is diffusion limited versus reaction rate limited. Although the constituent level diffusivities of the composite are assumed to be isotropic, the geometry of the unidirectional composite results in effective diffusivities that are transversely isotropic. Thus, in order to establish the relationship between the homogenized diffusivities of the oxidized composite and

the observed oxidation layer size, we calculate the ratio of the oxidation layer size in the composite in the axial direction (t_{axial}) to that in the transverse direction (t_{trans}) and as a first approximation compare it with the corresponding ratio of homogenized diffusivities of the composite. The composite effective diffusivities were recently calculated [27] using homogenization theories for various ratios of D_f/D_m and are listed in Table 4. Here D_1 and D_2 denote the effective axial and transverse diffusivities, respectively, of the unidirectional composite. Table 4 also shows a comparison of the anisotropy ratio of the diffusivities ($D_1/D_{2)}$ with the corresponding oxidation layer ratio (t_{axial}/t_{trans}) and the reaction zone ratio (l_{axial}/l_{trans}) at 200 hours simulations for some selected fiber and matrix diffusivity values. For values of $D_f/D_m < 10$, the oxidation growth is diffusion limited and the diffusivity factor obtained from the homogenization method closely matches the observed anisotropy in the oxidation layer sizes. However for larger ratios of D_f/D_m (i.e., >10), the oxidation process is observed to become reaction rate limited as the reaction zone ratio also increases with increasing D_f/D_m ratio. The oxidation layer ratio t_{axial}/t_{trans} therefore is calculated to be less than the corresponding D_1/D_2 diffusivity factor since oxidation is not occurring as rapidly as the rate at which oxygen is being supplied. Hence a larger portion of the surface layer now has regions in which complete oxidation has not occurred, leading to an increase in the size of the "active" reaction zone.

In earlier discussion, we had suggested that the diffusivity of carbon fibers will likely be anisotropic in nature since the extruded PAN carbon fibers exhibit a preferred orientation. To examine this, we simulated the oxidation growth with several assumed values of fiber axial and transverse diffusivity values denoted by $D_{f,axial}$ and $D_{f,trans}$

respectively, and compared the solution with the corresponding isotropic fiber case. Table 5 lists the results of our simulations. As an example, an isotropic fiber with $D_f = 0.1\ D_m^{ox}$ produces a t_{axial}/t_{trans} value of 1.31 (t_{axial}= 57.5 μm , t_{trans} = 43.9 μm) and with $D_f = 10\ D_m^{ox}$ produces 1.56 (t_{axial}= 122.5 μm , t_{trans}= 78.56 μm). In comparsison, an anisotropic fiber with $D_{f,axial} = 10\ D_m^{ox}$ and $D_{f,trans} = 0.1\ D_m^{ox}$ produces a t_{axial}/t_{trans} value of 4.41 after 200 hours of oxidation (t_{axial}= 193.75 μm , t_{trans} = 43.9 μm). Thus, the simulations show that anisotropy in fiber diffusivity can lead to larger oxidation layer ratio in unidirectional composites. Similar trends are observed for other diffusivity values as seen in Table 5. However, the extent of anisotropy seen in the simulations is not as much as that seen in experimental observations of oxidation growth in G30-500/PMR-15 composites where the ratio $(t_{axial}+l_{axial})/(t_{trans}+l_{trans})$ approaches nearly eight.

4.3 RVE with Interphase Layers

To investigate the role of the interphase region, particularly if the interphase thickness and its diffusivity are large, a study is conducted to understand the influence of the interphase parameters on the oxygen diffusivity and transport in the composite. This is accomplished by extending the RVE analysis to include a finite thickness interphase layer. The interphase layer is assumed to be a concentric cylinder with that of the fiber with a thickness of 5% that of the fiber radius. We assume the fiber diffusivity to be isotropic and set it equal to $0.1\ D_m^{ox}$, while the diffusivity of the interphase is assumed to be anisotropic, with axial diffusivity $D_{i,axial} = 10\ D_m^{ox}$ and transverse diffusivity $D_{i,trans} = D_m^{ox}$. Fig. 17 shows the comparison of the oxidation layer growth

within an RVE which includes the interphase with another RVE in which no interphase is present at various time intervals (10, 20 and 30 hours). Clearly, the presence of a highly diffusive interphase region contributes to an increase in the oxidation layer growth transverse to and in the fiber direction. The evidence of higher diffusivity in the axial direction compared to that in transverse direction can also be found in the sizes of the active reaction zones. Next, for results shown in Table 6, we set the fiber diffusivity at 0.1 D_m^{ox} while the interphase diffusivity values are varied. The first row in Table 6 is the result at 200 hours simulation with no interphase region. We observe that the addition of a highly diffusive anisotropic interphase results in substantial increase in composite oxidation in the axial direction, while only small changes occur in oxidation region in the transverse direction. Thus, similar to the fiber anisotropy, the simulations show that anisotropy in interphase diffusivity can also lead to larger oxidation layer ratio in unidirectional composites.

4.4 Modeling with Damage Evolution at the Interphase

Our modeling results so far indicate that the experimentally observed extent of anisotropy in the oxidation growth cannot be explained with rational choices for fiber and interphase diffusivities alone. The rapid oxidation rate along the fiber length indicates that a degradation process is creating oxygen diffusion paths deep into the specimen, possibly in the form of fiber-matrix debonding. In order to simulate the effect of interphase damage on the oxidation layer size, an oxidation state dependent damage evolution model can be formulated by extending the basic framework of the matrix oxidation model. The damage evolution itself can be considered to be similar to

that of the oxidation reaction and consumption model where in the interphase's damage state can be tracked by a damage state parameter (ϕ_d). The damage process can be controlled by the presence of oxygen (through the oxygen concentration variable, c(x,y,z,t)) and a reaction rate process, $R_i(C)$. The damage process can therefore be analogous to subtrate conversion in the oxidation simulation and the rate can be controlled by a conversion parameter, α_d which will be analogous to the subtrate conversion rate parameter α. Next, a diffusivity to damage relation will have to be assumed for the interphase region. As the damage state of the material will change from undamaged to damaged, the diffusivity of the interphase can be altered in the simulation. This will allow the damage and the thermo-oxidation processes to follow independent rate kinetics as we simulate the effect of damage on the thermo-oxidation.

5. Summary

Thermo-oxidative degradation of PMCs is clearly a subject of major importance as designers push the high temperature endurance limits of polymer composites to improve the performance of aerospace systems. Along with all of the tremendous challenges of modeling the performance and strength of composites in benign thermal environments, are added the difficult challenges of modeling the age-dependent properties of composites at high temperature. The strong interaction of the physical, chemical, and mechanical aging behavior of HTPMCs is due to the significant contrast in the properties of the fiber and matrix constituents of the composite. These interactions are particularly apparent in the critical fiber-matrix interface/interphase where the

interface/interphase has been shown to play a dominant role in the thermo-oxidation process.

In this work, an overview of the experimentally observed thermo-oxidative behavior of PMR-15 neat polymer and carbon fiber/PMR-15 composites has been presented along with a theoretical treatment of oxidation development. Literature search indicates that although the degradation of the in-situ fiber in the composite has long been considered to be negligible, the role of the fiber and its contribution to the oxidation process has not been fully explored. Specifically, little is known about the diffusivity of oxygen in the fiber and its contribution to the transport of oxygen to the interior of the composite. A method for high resolution oxidation modeling capable of simulating thermo-oxidation for composites with multiple phases and anisotropic diffusivity has been developed. The new method utilizes a diffusion/reaction model in which temperature, oxygen concentration, and weight loss effects are considered. Three dimensional FEM analyses have been used to demonstrate the interactions between fiber and resin in PMCs. Parametric studies illustrating the anisotropy in the oxidative region growth and the effect of fiber and interphase diffusivity on the oxidation layer growth rates are discussed. It is suggested that alternative pathways for transport of oxygen into the interior of the composite are fiber-matrix debonds that propagate with the oxidation front. This possible mechanism for accelerated oxidation along the composite fiber direction is an excellent example of the intrinsic coupling of chemical oxidative aging and damage. Whereas cracks can accelerate oxidation by providing pathways for oxidants, so can oxidation lead to cracking in the resin matrix and at fiber-

matrix interfaces. The critical nature of the fiber-matrix interphase on degradation and failure processes in composites signifies the importance of proper representation of its behavior in predictive models. Since failure initiation is typically associated with the fiber-matrix interface/interphase region, the importance of modeling the coupling effects of damage and oxidation cannot be over emphasized.

Simulations have compared well with experimental data, but further refinement is still necessary. While it is only one mechanism in the aging process of PMCs, successful simulation of thermo-oxidation behavior is a critical part of understanding this complex process and in providing a foundation for understanding the mechanisms of degradation for long-term environmental exposure and loading.

6. Acknowledgements

This work is supported by the Air Force Office of Scientific Research under the Materials Engineering for Affordable New Systems (MEANS) program sponsored by Dr. Charles Lee. Particular thanks are due to Stevens Institute of Technology students (Eva Yu and Harold Cook) for numerical analyses.

7. References

1. X. Colin, J. Verdu, Compos. Sci. Technol. 65 (2005) 411-419.
2. X. Colin, A. Mavel, C. Marais, J. Verdu, J. Compos. Mat. 39 (2005) 1371-1389.
3. S. S. Wang, X. Chen, J. Eng. Mat. Technol. 128 (2006) 81-89.
4. K. V. Pochiraju, G. P. Tandon, J. Eng. Mat. Technol. 128 (2006) 107-116.
5. G. P. Tandon, K. V. Pochiraju, G. A. Schoeppner, Polymer Degrad. Stability 91 (2006) 1861-1869.
6. A. Skontorp, M. S. Wong, S. S. Wang, High-temperature anisotropic thermal oxidation of carbon-fiber reinforced polyimide composites. Theory and experiment. In:Proceedings of ICCM-10, Whistler B.C., Canada (1995) IV:375
7. J. Wise, K. T. Gillen, R. L. Clough, Polymer, 38 (1997) 1929-44.
8. H. L.McManus, B. J. Foch, R. A. Cunningham, J Comp. Tech. Res. 22 (2000) 146-152
9. K. J. Bowles, D. S. Papadopoulos, L. L. Inghram, L. S. McCorkle, O. V. Klan, NASA/TM-2001-210602, 2001.

10. L. C. Tsuji, H. L. McManus, K. J. Bowles, NASA Technical Report, 1998-208487, 1998.
11. K. Abdeljaoued, Thermal oxidation of PMR-15 polymer used as a matrix in composite materials reinforced with carbon fibers. MS thesis, Ecole Nationale Superieure des Arts et Metiers, Paris, 1999.
12. G. A. Schoeppner, G. P. Tandon, E. R. Ripberger, Composites Part A: Appl. Sci. Manufacturing 38 (2007) 890-904.
13. M. A. Meadors, C. E. Lowell, P. J. Cavano, P. Herrera-Fierro, High Perf. Polymers 8 (1996) 363-379.
14. E. R. Ripberger, G. P. Tandon, G. A. Schoeppner, Characterizing oxidative degradation of PMR-15 resin. In: Proceedings of the Spring SAMPE 2004 Symposium/Exhibition, Long Beach, CA (2004)
15. S. Ciutacu, P. Budrugeac, I. Niculae, Polymer Degrad. Stability 31 (1991) 365-372.
16. T. K. Tsotsis, S. Keller, J. Bardis, J. Bish, Polymer Degrad. Stability 64 (1999) 207-212.
17. G. P. Tandon, E. R. Ripberger, G. A. Schoeppner, Accelerated aging of PMR-15 resin at elevated pressure and/or temperature. In: Proceedings of the SAMPE 2005 Symposium and Exhibit, Seattle, WA (2005).
18. B. H. Eckstein, Fiber Sci. Technol. 14 (1981) 139-156.
19. H. H. Gibbs, R. C. Wendt, F. C. Wilson, Polymer Eng. Sci. 19 (1979) 342-349.
20. G. P. Tandon, J. Briggs, G. A. Schoeppner, Thermo-oxidative degradation of carbon fibers for high-temperature polymer matrix composites. In: Proceedings American

Society for Composites, 21st Technical Conference, Univ. of Michigan-Dearborn, Dearborn, MI (2006).

21. J. B. Nelson, Thermal aging of graphite polyimide composites. In: O'Brien TK, editor, Long-Term Behavior of Composites, ASTM STP 813: American Society for Testing and Materials, Philadelphia, (1983) pp 206-221
22. J. D. Nam, J. C. Seferis, SAMPE Quart. 24 (1992) 10-18.
23. K. J. Bowles, A. Meyers, Specimen geometry effects on graphite/PMR-15 composites during thermo-oxidative aging. In: Proceedings 31st International SAMPE Symposium, Covina, CA (1986) 1285-1299.
24. X. Colin, J. Verdu, Plastics, Rubber and Composites 32 (2003) 349-356.
25. X. Colin, C. Marais, J. Verdu, Polymer Testing 20 (2001) 795-803.
26. L. Q. Tang, K. V. Pochiraju, C. Chassapis, S. Manoocheri, Int. J. Num. Meth. Engrg., 39 (1996) 3049-3064.
27. K. V. Pochiraju, H. Cook, G. P. Tandon, G. A. Schoeppner, Modeling Thermo-Oxidation in High Temperature Polymer Matrix Composites. In: Proceedings American Society for Composites, 21st Technical Conference, Univ. of Michigan-Dearborn, Dearborn, MI (2006).

Table Captions

Table 1 Diffusivity parameters for PMR-15 resin

Table 2 Reaction rate parameters for PMR-15 resin

Table 3 Weight loss model parameters for PMR-15 resin

Table 4 Anisotropy in composite diffusivity and its correlation with oxidation layer size

Table 5 Influence of fiber anisotropy on composite oxidation

Table 6 Influence of interphase region on composite oxidation

Figure Captions

Fig. 1. Oxidation measurement procedures

Fig. 2. Photomicrograph of PMR-15 resin showing the formation of oxidized region

Fig. 3. Evolution of oxidation layer and transition region thickness with aging time in PMR-15 resin at 288^0C

Fig. 4. Oxidation layer thickness for ambient and elevated pressure aging in PMR-15

Fig. 5. Normalized weight loss of G30-500 fiber and PMR-15 resin

Fig. 6. (a) Array of eight stitched photomicrographs of oxidized specimen cross section, (b) Enhanced micrograph of the specimen cross section

Fig. 7. Unidirectional G30-500/PMR-15 composite at 407, 1200 and 2092 hours of oxidation at 288ºC

Fig. 8. Comparison of oxidation growth in axial and transverse directions of composite

Fig. 9. Comparison of oxidation growth in transverse direction of composite and in neat resin PMR-15

Fig. 10. Schematic of the three-zones in thermo-oxidation.

Fig. 11. Prediction of oxidation thickness at 316°C and 343°C based on 288°C model parameters

Fig. 12. Influence of sorption on the oxidation layer thickness

Fig. 13. Prediction of oxidation thickness for pressurized aging of PMR-15

Fig. 14. User input interface for TOM-3D

Fig. 15. Representative volume elements used for the analyses (a) Single Fiber RVE (12.5 μm x 12.5 μm x 125 μm) with one surface exposed to oxidation; (b) Ten Fiber RVE (125 μm x 12.5 μm x 125 μm) with both axial and transverse directions exposed to oxidation.

Fig. 16: Effect of fiber diffusivity on composite oxidation. Black regions are completely oxidized and grey regions are unoxidized. The transition region is contoured from black to grey based on the oxidation state. All dimensions shown are in μm. (a) $D_f = 0.01\ D_m^{ox}$, (b) $D_f = 0.1\ D_m^{ox}$, (c) $D_f = 10\ D_m^{ox}$

Fig. 17. Effect of a highly diffusive fiber-matrix interphase region. The anisotropy in the oxidation layer can be clearly seen.

Table 1

Diffusivity parameters for PMR-15 resin

	Unoxidized, $\phi = 1$	Oxidized, $\phi = \phi_{ox}$
D_0	6.10×10^{-11} m^2/sec	8.90×10^{-11} m^2/sec
E_a	19,700 J/mol	
R	8.31447 J/(mol ºK)	

Table 2

Reaction rate parameters for PMR-15 resin

Parameter	Value
$R_0^{'}$	536.94 mol/(m^3.min)
R_a	23379.63 J/mol
β	0.92 m^3/mol

Table 3

Weight loss model parameters for PMR-15 resin

Parameter	Value
α	0.01-(0.01-.0033)*t/40 m^3/mol, t < 40 hrs 0.0033 m^3/mol, t > 40 hrs
ϕ_{ox}	0.18

.

Table 4

Anisotropy in composite diffusivity and its correlation with oxidation layer size

Diffusivity/D_m^{ox}		Diffusivity Factor			Predicted Oxidation Layer Size Ratio (t_{axial}/t_{trans})	Predicted Reaction Zone Size Ratio (l_{axial}/l_{trans})
Matrix	Fiber	D_1/D_m^{ox}	D_2/D_m^{ox}	D_1/D_2		
1	0.1	0.551	0.415	1.33	1.31	1.15
	2	1.499	1.4	1.07	1.20	0.83
	4	2.34	1.653	1.42	1.43	0.95
	10	5.49	2.41	2.28	1.56	2.00
	20	10.48	2.69	3.89	2.71	2.68
	46	23.45	2.89	8.11	3.25	3.5
	60	30.52	2.91	10.49	3.45	3.93
	100	50.37	2.99	16.84	4.41	5.39
	200	100.5	3.015	33.33	7.40	10.53

Table 5

Influence of fiber anisotropy on composite oxidation

$D_{f,\,axial}/D_m^{ox}$	$D_{f,\,trans}/D_m^{ox}$	t_{axial}, μm	l_{axial}, μm	t_{trans}, μm	l_{trans}, μm	t_{axial}/t_{trans}	l_{axial}/l_{trans}	$(t_{axial} + l_{axial})/(t_{trans} + l_{trans})$
0.1	0.1	57.5	23.75	43.9	20.6	1.31	1.15	1.26
10	10	122.5	75	78.56	37.41	1.56	2.0	1.57
10	0.1	193.75	106.25	43.9	20.63	4.41	5.15	4.65
2	1	85	40	64.06	26.45	1.33	1.51	1.38
2	2	78.75	38.75	65.47	46.82	1.20	0.83	1.05
4	1	107.5	72.5	65.47	42.09	1.64	1.72	1.67
4	4	92.5	48.8	64.53	51.37	1.43	0.95	1.22
10	1	185	78	61.72	31.8	3.0	2.45	2.81
10	10	122.5	75	78.56	37.41	1.56	2.0	1.57
20	1	257	112	57.98	29.93	4.43	3.74	4.20
20	20	150	100	55.25	37.25	2.71	2.68	2.70

Table 6: Influence of interphase region on composite oxidation

$D_{i,axial}/D_m^{ox}$	$D_{i,trans}/D_m^{ox}$	t_{axial}, μm	l_{axial}, μm	t_{trans},μm	l_{trans}, μm	t_{axial}/t_{trans}	l_{axial}/l_{trans}
-	-	57.5	23.75	43.9	20.6	1.31	1.15
1	1	59.14	22.18	47.74	23.87	1.24	0.93
10	1	95.43	32.26	49.23	22.38	1.94	1.44

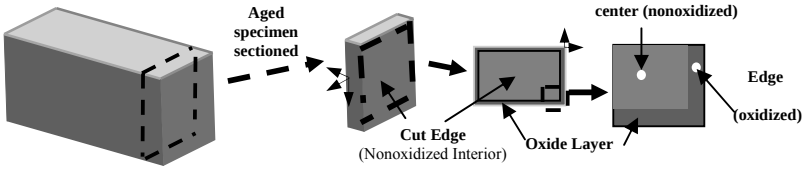

Fig. 1. Oxidation measurement procedures

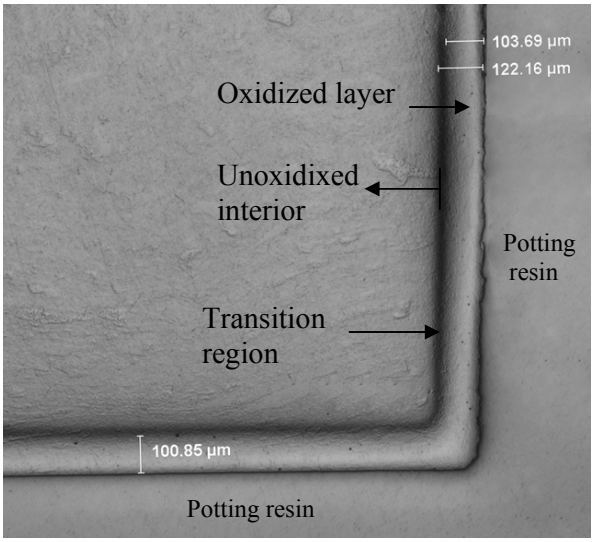

Fig. 2. Photomicrograph of PMR-15 resin showing the formation of oxidized region

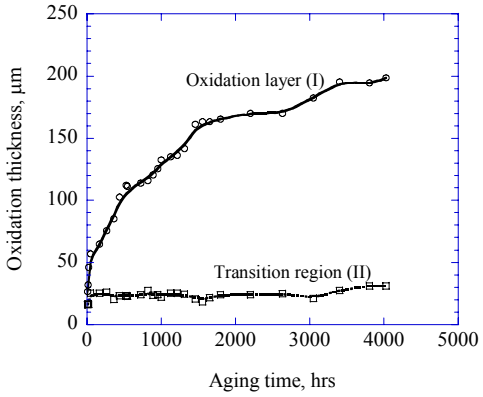

Fig. 3. Evolution of oxidation layer and transition region thickness with aging time in PMR-15 resin at 288^0C

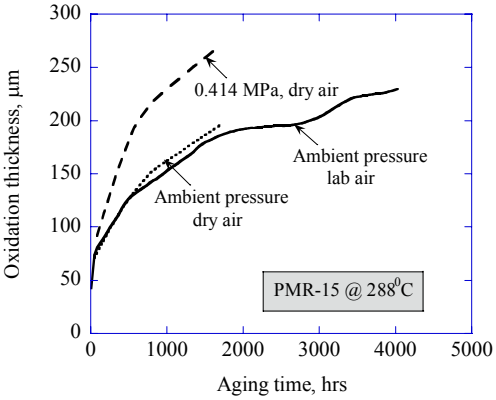

Fig. 4. Oxidation layer thickness for ambient and elevated pressure aging in PMR-15

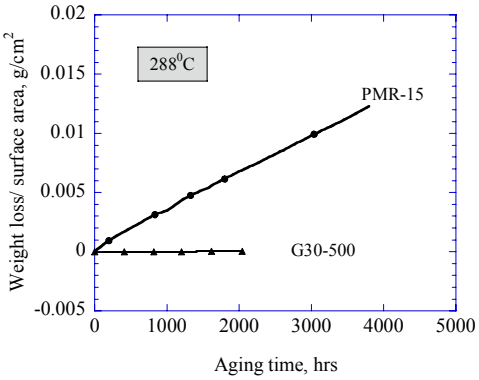

Fig. 5. Normalized weight loss of G30-500 fiber and PMR-15 resin

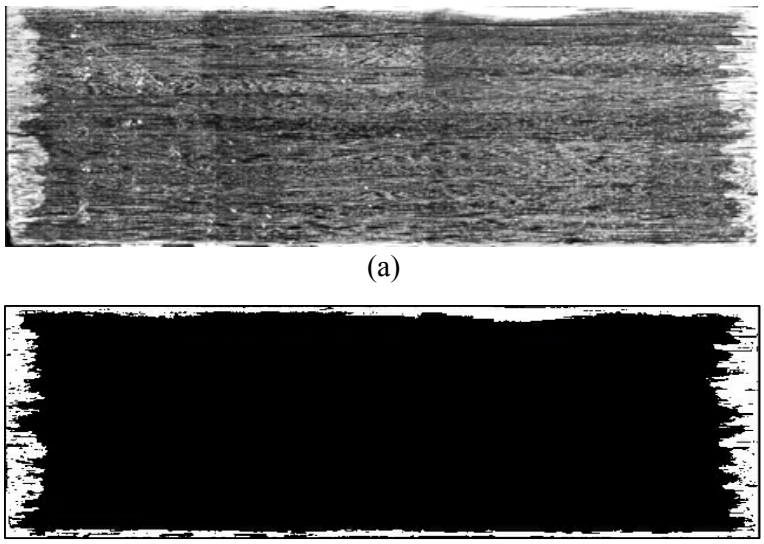

(a)

(b)

Fig. 6. (a) Array of eight stitched photomicrographs of oxidized specimen cross section,

(b) Enhanced micrograph of the specimen cross section

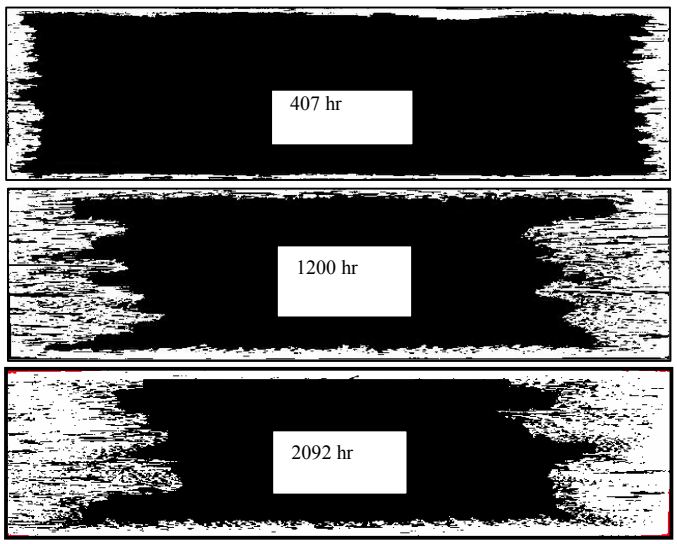

Fig. 7. Unidirectional G30-500/PMR-15 composite at 407, 1200 and 2092 hours of oxidation at 288ºC

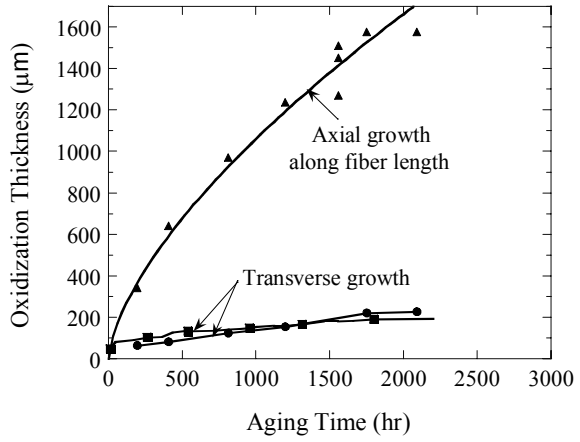

Fig. 8. Comparison of oxidation growth in axial and transverse directions of composite

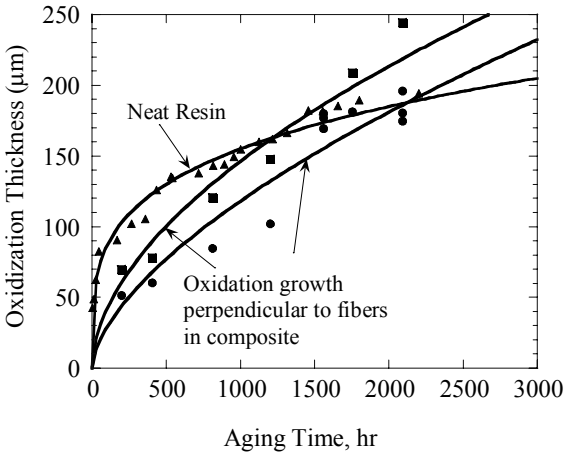

Fig. 9. Comparison of oxidation growth in transverse direction of composite and in neat resin PMR-15

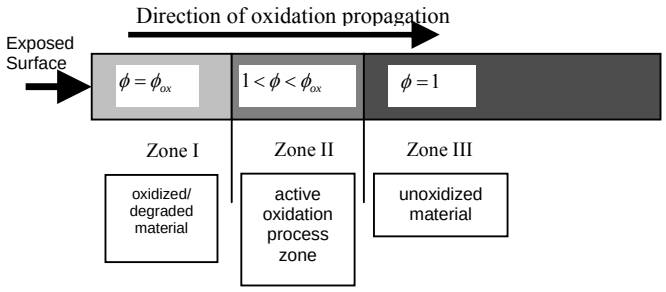

Fig. 10. Schematic of the three-zones in thermo-oxidation.

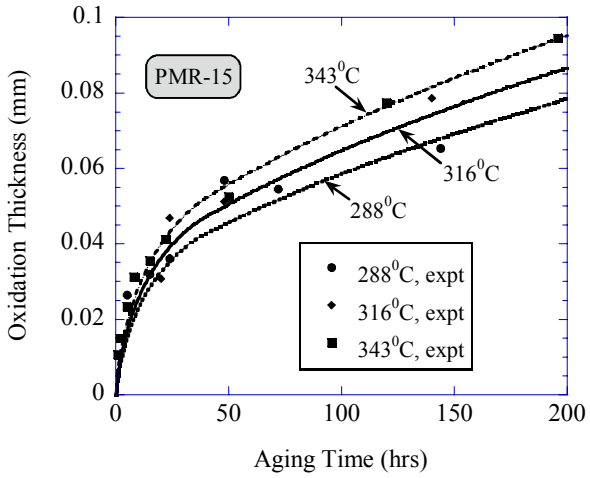

Fig. 11. Prediction of oxidation thickness at 316°C and 343°C based on 288°C model parameters

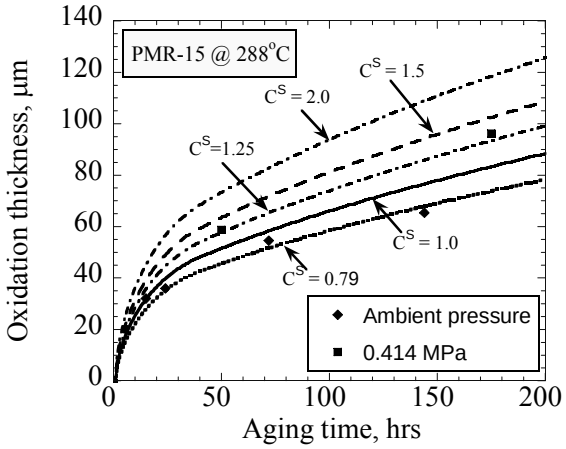

Fig. 12. Influence of sorption on the oxidation layer thickness

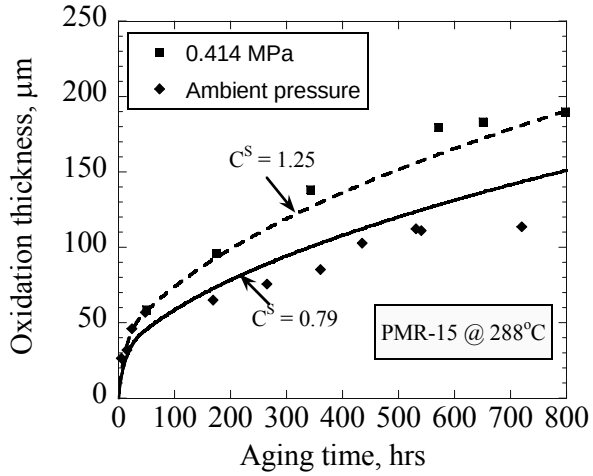

Fig. 13. Prediction of oxidation thickness for pressurized aging of PMR-15

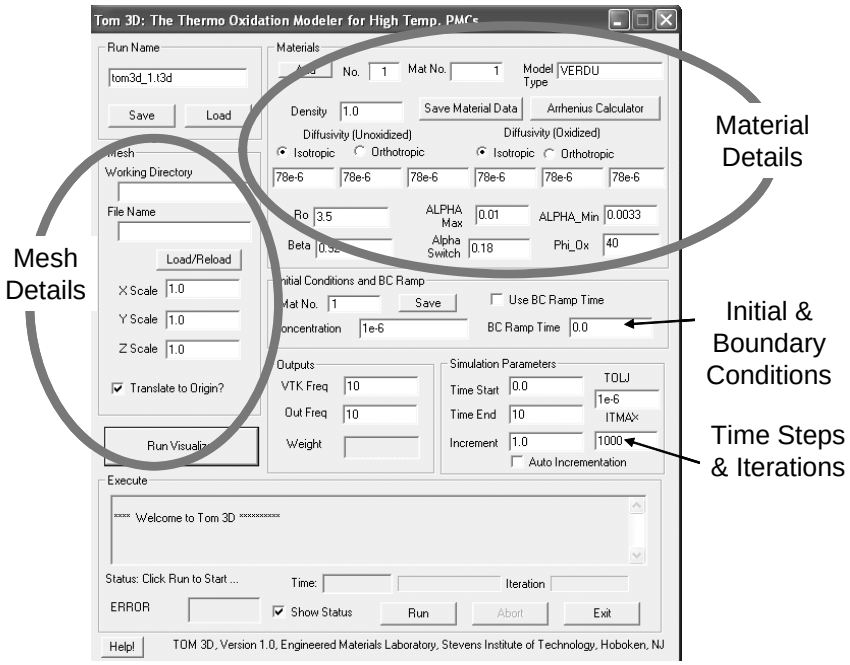

Fig. 14. User input interface for TOM-3D

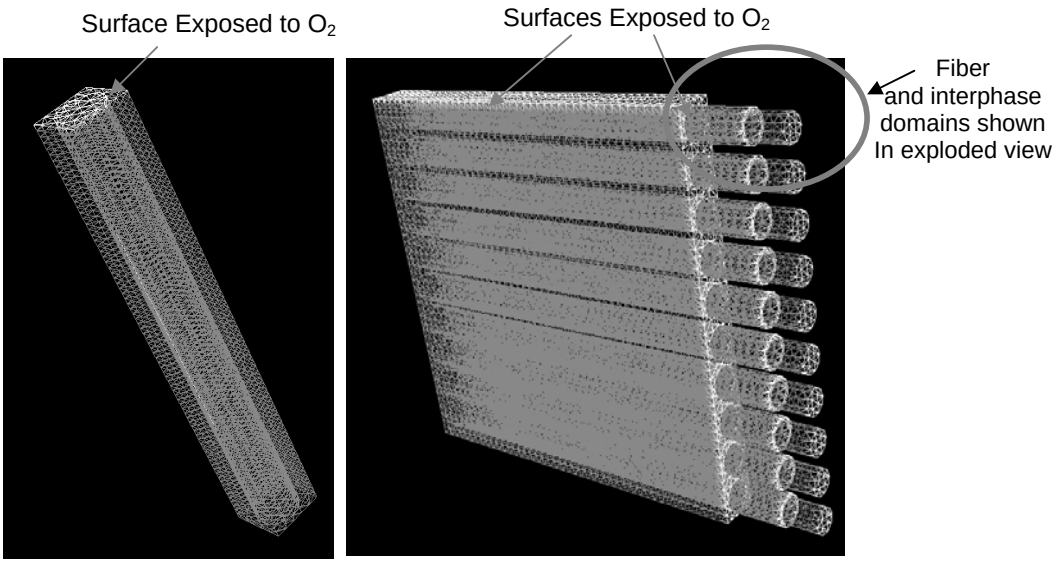

(a) (b)

Fig. 15. Representative volume elements used for the analyses
(a) Single Fiber RVE (12.5 μm x 12.5 μm x 125 μm) with one surface exposed to oxidation; (b) Ten Fiber RVE (125 μm x 12.5 μm x 125 μm) with both axial and transverse directions exposed to oxidation.

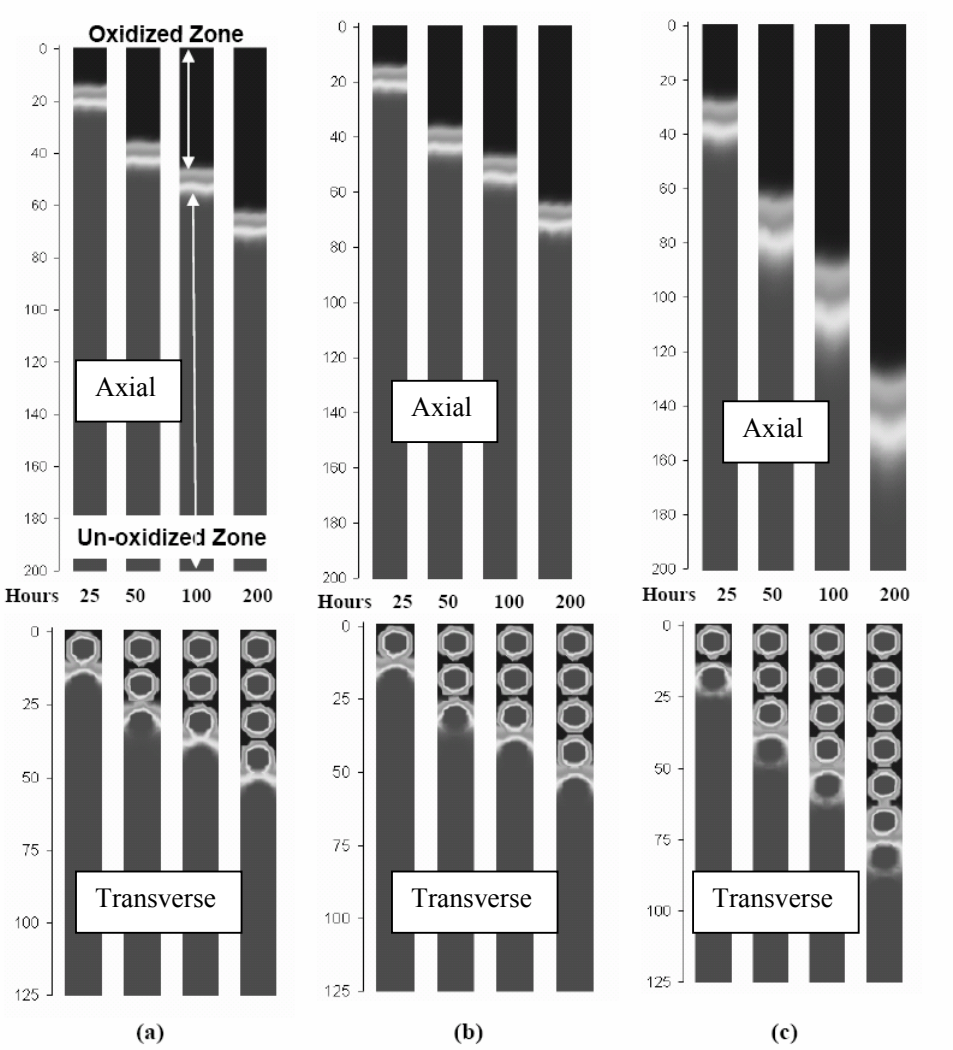

Fig. 16: Effect of fiber diffusivity on composite oxidation. Black regions are completely oxidized and grey regions are unoxidized. The transition region is contoured from black to grey based on the oxidation state. All dimensions shown are in μm.

(a) $D_f = 0.01\ D_m^{ox}$, (b) $D_f = 0.1\ D_m^{ox}$, (c) $D_f = 10\ D_m^{ox}$

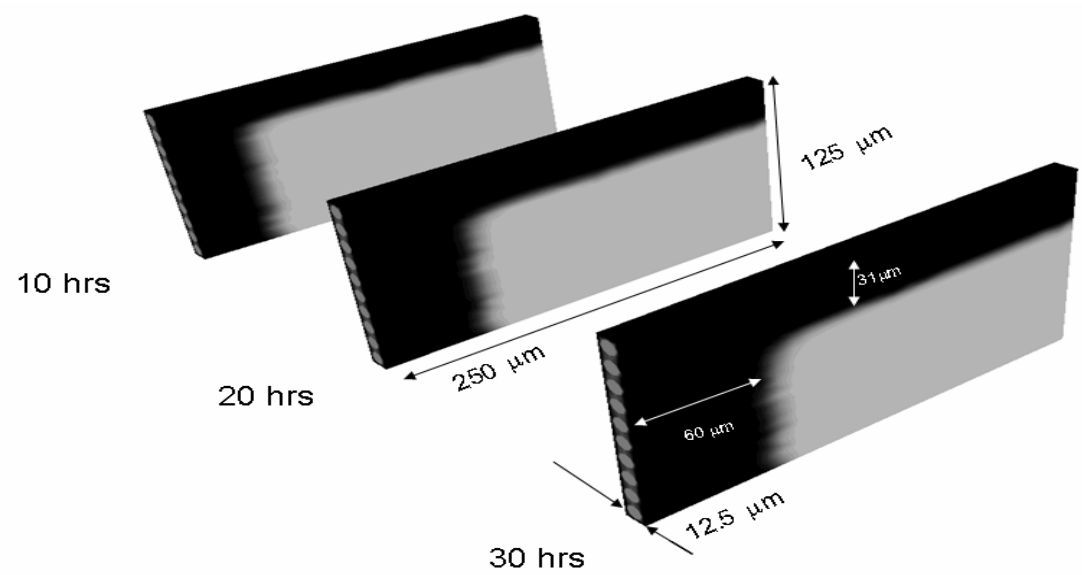

With Interphase ($D_f = 0.1\ D_m^{ox}$; $D_{i,\,axial} = 10\ D_m^{ox}$; $D_{i,trans} = D_m^{ox}$) : $t_{axial}/t_{trans} = 1.935$

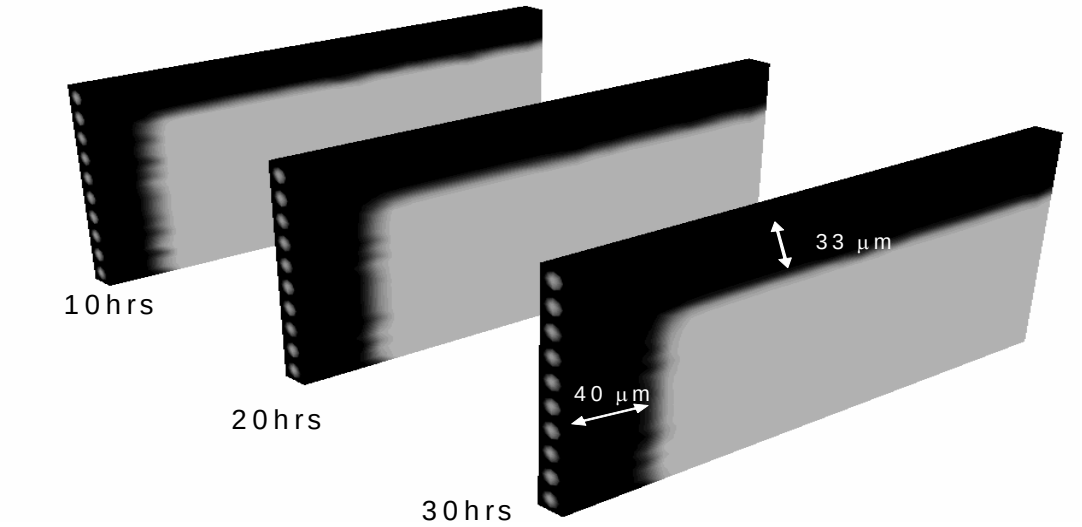

No Interphase ($D_f = 0.1\ D_m^{ox}$); $t_{axial}/t_{trans} = 1.212$

Fig. 17. Effect of a highly diffusive fiber-matrix interphase region. The anisotropy in the oxidation layer can be clearly seen.